Appl. Phys. A
DOI 10.1007/s00339-014-8390-7

Applied Physics A
Materials Science & Processing

Characterization of Al/Si junctions on Si(100) wafers with chemical vapor deposition-based sulfur passivation

Hai-feng Zhang · Arunodoy Saha · Wen-cheng Sun · Meng Tao

Received: 13 November 2013 / Accepted: 11 March 2014

Abstract Chemical vapor deposition-based sulfur passivation using hydrogen sulfide is carried out on both n-type and p-type Si(100) wafers. Al contacts are fabricated on sulfur-passivated Si(100) wafers and the resultant Schottky barriers are characterized with current–voltage (*I–V*), capacitance–voltage (*C–V*) and activation-energy methods. Al/S-passivated n-type Si(100) junctions exhibit ohmic behavior with a barrier height of <0.078 eV by the *I–V* method and significantly lower than 0.08 eV by the activation-energy method. For Al/S-passivated p-type Si(100) junctions, the barrier height is ~0.77 eV by *I–V* and activation-energy methods and 1.14 eV by the *C–V* method. The discrepancy between *C–V* and other methods is explained by image force-induced barrier lowering and edge-leakage current. The *I–V* behavior of an Al/S-passivated p-type Si(100) junction remains largely unchanged after 300 °C annealing in air. It is also discovered that heating the S-passivated Si(100) wafer before Al deposition significantly improves the thermal stability of an Al/S-passivated n-type Si(100) junction to 500 °C.

1 Introduction

Among the many techniques for surface passivation on Si, thermal oxidation of Si provides arguably the best-quality passivation [1–3]. Si nitride (SiN_x) by plasma-enhanced chemical vapor deposition is widely used in Si photovoltaic solar cells for both surface passivation and antireflection [4, 5]. A recent development in surface passivation for Si solar cells is Al oxide (Al_2O_3) by atomic layer deposition, in which the negative charges provide excellent passivation for p-type Si surface [6, 7]. Although these techniques have been proven effective, the insulating layers prevent metallization on the passivated surface for electrical contacts. The concept of "valence-mending" was proposed by Kaxiras to terminate dangling bonds on the Si(100) surface [8]. A valence-mended Si(100) surface by a single atomic layer of sulfur (S) or selenium(Se) has led to record-low and record-high Schottky barriers. Tao et al. reported an record-low Schottky barrier of 0.08 eV for an Al/Se-passivated n-type Si(100) junction using molecular beam epitaxy (MBE) for passivation [9]. Although the quality of MBE passivation is superior, its high cost and low throughput prevent its practical applications. Song et al. demonstrated a record-high Schottky barrier of 1.1 eV for an Al/S-passivated p-type Si(100) junction using solution passivation [10]. The solution method is advantageous on cost and throughput, but the quality of solution passivation is far inferior to that of MBE passivation. This is evidenced by the poor thermal stability of the record-high Schottky barrier [10] and prevents its practical applications.

Chemical vapor deposition (CVD) is considered as the best candidate for valence-mending passivation, which provides good passivation quality, low process cost and high throughput. Furthermore, CVD allows both sides of a wafer to be passivated simultaneously when the wafer sits upright. CVD also allows valence-mending passivation of Si(111) surface such as textured Si(100) wafers with (111) facets in Si solar cells. The dangling bonds on Si(111) points perpendicular to the surface at one dangling bond per surface atom requires Group VII atoms such as fluorine or chlorine (Cl) to terminate. Group VII precursors such as

H. Zhang (✉) · A. Saha · W. Sun · M. Tao
School of Electrical, Computer and Energy Engineering, Arizona State University, PO Box 875706, Tempe, AZ 85287, USA
e-mail: Haifeng.zhang@asu.edu

M. Tao
e-mail: meng.tao@asu.edu

Published online: 26 March 2014

hydrogen chloride (HCl) are readily available for such a CVD process.

In this paper, CVD-based sulfur passivation is carried out on both n-type and p-type Si(100) wafers. Al contacts are fabricated on S-passivated Si(100) wafers and electrical characterization of the Al/S-passivated Si(100) junctions is performed. The barrier height of Al/S-passivated n-type Si(100) junctions is found to be significantly lower than that of Al/Se-passivated n-type Si(100) junctions using MBE passivation. For Al/S-passivated p-type Si(100) junctions, capacitance–voltage measurements suggest a barrier height of 1.14 eV, which is larger than the bandgap of Si.

2 Experimental details

For the experiment, 4-inch n-type Si(100) wafers with $\sim 1\times10^{16}$ cm^{-3} phosphorous doping and p-type Si(100) wafers with $\sim 2\times10^{16}$ cm^{-3} boron doping were used. The wafers were first cleaned in 2 % hydrogen fluoride (HF) for 30 s and subsequently dried with nitrogen. The wafers were then loaded into a CVD reactor through a load lock. The pressure of the reactor was pumped to a base vacuum of 2×10^{-8} Torr and then the temperature of the reactor was ramped up to 750 °C. Sulfur passivation was carried out by introducing high-purity hydrogen (H_2), HCl and hydrogen sulfide (H_2S) into the reactor. The flow rates of H_2, HCl and H_2S for passivation were 10 sccm each. H_2 serves as the carrier gas and also helps clean the surface. HCl plays a critical role in removing surface contamination such as metals from the Si wafer. H_2S is the sulfur precursor for valence-mending passivation of Si(100) surface. During passivation, the temperature of the reactor was ramped down from 750 to 150 °C, and HCl, H_2S and H_2 were sequentially stopped around 150 °C. The wafer was unloaded when the reactor temperature was below 100 °C.

After passivation, Al contacts with thickness of 100 nm and diameter of 216 μm were deposited on the wafer by electron-beam evaporation at a base vacuum of 5×10^{-6} Torr through a shadow mask. The shadow mask contains hundreds of holes, allowing many Al/Si junctions in one experiment to obtain reliable and averaged results. With good-quality passivation, the measured results are fairly consistent. For this reason, one Al contact was randomly chosen for all the electrical measurements presented here. Al was also deposited on the entire backside of the wafer as the back contact. Although the back contact is Schottky, the large area of the back contact (10^5 times larger than the front contact) makes it possible to characterize the front Al/Si junctions without the Schottky effect from the back contact. In some cases the Al/S-passivated Si junctions were characterized through two adjacent Al contacts on the front side, which is equivalent of measuring two back-to-back Schottky junctions. Only one pair of Al contacts was randomly chosen for all the measurements presented here. For comparison, Al contacts were also fabricated on Si(100) wafers from the same batch but without sulfur passivation. These control wafers were cleaned in 2 % HF for 30 s which provided H-passivated surface. Current–voltage (I–V), capacitance–voltage (*C–V*) and activation-energy measurements were performed to determine the Schottky barrier height. For low Schottky barriers (Al/S-passivated n-type Si(100) junctions), activation-energy measurements were carried out between 77 K (liquid nitrogen) and room temperature (300 K). For high Schottky barriers (Al/S-passivated p-type Si(100) junctions), the temperature range in activation-energy measurements was 300 K–400 K.

To determine if edge-leakage current was present in Al/S-passivated p-type Si(100) junctions, Al contacts with various diameters were deposited on a S-passivated p-type Si(100) wafer by electron-beam evaporation through a shadow mask. The diameters of the Al contacts were from 600 to 1,200 μm. Al was also deposited on the backside of the wafer as the back contact, and *I–V* measurements were performed between a front Al contact and the back Al contact. To determine the thermal stability of sulfur passivation, Al/S-passivated p-type Si(100) junctions were annealed on a hotplate in air for 30 s at 300 °C, and their *I–V* behaviors before and after annealing were compared. For Al/S-passivated n-type Si(100) junctions, the deposition of Al contacts was performed at a substrate temperature of 220 °C in the electron-beam evaporator. Their *I–V* behaviors immediately and 47 days after fabrication, and then annealed on a hotplate in air for 30 s at different temperatures from 300 to 500 °C, were compared.

3 Results and discussion

3.1 Al/S-passivated n-type Si(100) junctions

By terminating dangling bonds on the Si(100) surface, a low Schottky barrier close to 0 eV is expected between Al and n-type Si [11]. Figure 1 shows the *I–V* characteristics between two adjacent Al contacts on S-passivated n-type Si(100) surface at different temperatures. The *I–V* characteristics between two Al contacts on a control n-type Si(100) wafer without sulfur passivation are included for comparison. It is noted that the *I–V* characteristics of a very low Schottky barrier can be overshadowed by a high series resistance. At room temperature, impedance spectroscopy indicates a practically constant series resistance of ~31 Ω, which prevents the calculation of the Schottky barrier height. In this case, *I–V* measurements of two back-to-back

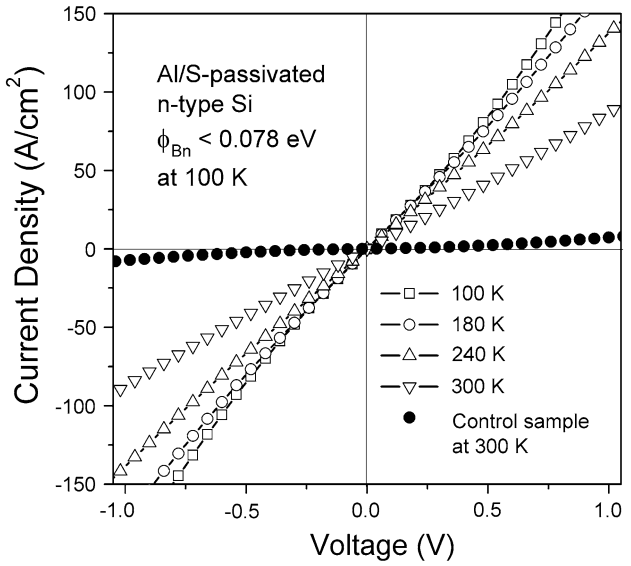

Fig. 1 I–V characteristics of Al/S-passivated n-type Si(100) junctions at different temperatures. *I–V* characteristics of Al/n-type Si(100) junctions without sulfur passivation are included for comparison

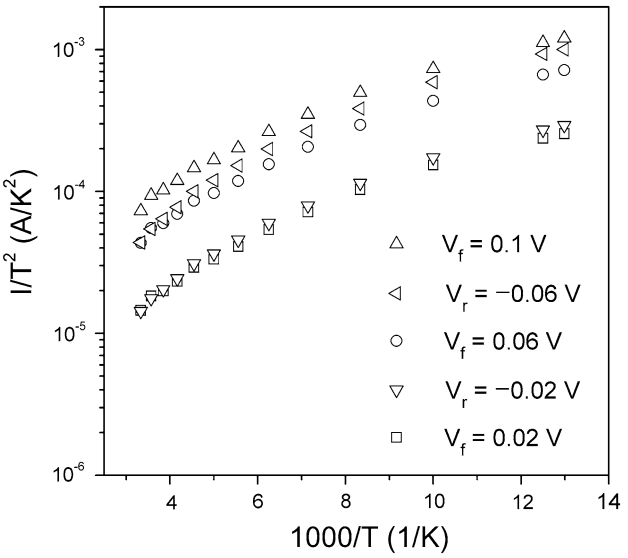

Fig. 2 Activation-energy measurements of an Al/S-passivated n-type Si(100) junction between 77 and 300 K and under different bias. The *positive slopes* indicate a very low Schottky barrier

Schottky junctions at low temperatures are proposed as the most effective method to evaluate the barrier height [12]. As shown in Fig. 1, the *I–V* characteristics are linear at temperatures as low as 100 K, suggesting a very low Schottky barrier. The thermionic emission model describes the *I–V* relationship of a Schottky junction as:

$$I = A_{\text{eff}} A^{**} T^2 e^{-q\phi_B/kT}\left[e^{q(V-IR)/nkT} - 1\right], \quad (1)$$

where $A_{\text{eff}} = 3.66 \times 10^{-4}$ cm^2 is the effective area of the contact, A^{**} is the effective Richardson constant, ϕ_B is the zero-bias barrier height, k the Boltzmann constant, T the absolute temperature, q the electron charge, V the applied voltage, R the series resistance and n the ideality factor. Assuming the effective Richardson constant A^{**} is 120 A/cm^2 K^2 for n-type Si, a barrier height ϕ_{Bn} of less than 0.078 eV is obtained by simply fitting the *I–V* relationship at 100 K with the thermionic emission model. This barrier height is in agreement with our previous report for MBE-based Se passivation, 0.08 eV [9]. For comparison, the barrier height measured for Al contacts on a control wafer without sulfur passivation is 0.39 eV. This is higher than the S-passivated sample but lower than the historical value for Al on n-type Si, 0.72 eV [13]. The discrepancy with the historical data is partially attributed to the high edge-leakage current in our samples, which will be discussed later in this paper.

Activation-energy measurements of an Al/S-passivated n-type Si(100) junction under different bias were performed from 77 to 300 K to confirm the low Schottky barrier. As shown in Fig. 2, the activation-energy method yields positive slopes, indicating a very low Schottky barrier. With a reasonable barrier height, the slope in an *I/T*^{2} versus *1/T* plot is negative. A positive slope was observed in activation-energy measurements of a very low Schottky barrier [9]. In that case, a positive slope appeared near room temperature. In Fig. 2 a positive slope occurs

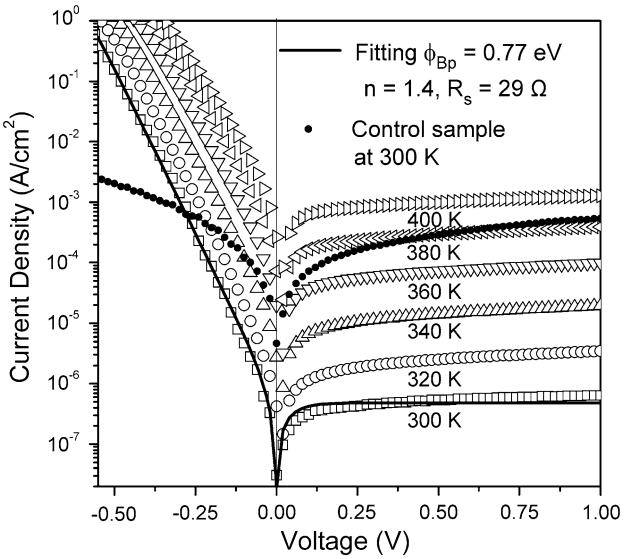

Fig. 3 I–V characteristics of an Al/S-passivated p-type Si(100) junction at different temperatures. *I–V* characteristics of an Al/p-type Si(100) junction without sulfur passivation are included for comparison

down to 77 K, suggesting a significantly lower Schottky barrier than our previous report, 0.08 eV. With the low Schottky barrier, the *C–V* method does not work.

3.2 Al/S-passivated p-type Si(100) junctions

Figure 3 shows the *I–V* characteristics of an Al/S-passivated p-type Si(100) junction at different temperatures from 300 to 400 K. The *I–V* characteristics for an Al contact on a control p-type Si(100) wafer without sulfur passivation are included for comparison. Assuming the effective Richardson constant A^{**} is 30 A/cm^2 K^2 for p-type Si, a barrier height ϕ_{Bp} of 0.77 eV is obtained by fitting the *I–V* relationship at 300 K with Eq. 1, along with a series resistance of 29 Ω and an ideality factor of 1.4. The series resistance mainly comes from the resistance of the Si wafer and the non-unity ideality factor may be attributed to the limitations of the thermionic emission model in high barrier measurements [14]. The barrier height on the control sample is 0.59 eV, which is in agreement with the historical value for Al on p-type Si, 0.58 eV [13].

Figure 4 is the activation-energy measurements on an Al/S-passivated p-type Si(100) junction under different bias between 300 and 400 K. Under forward bias of 0.2 V, the barrier height determined from the slope is 0.78 eV, which is in good agreement with the value obtained from *I–V* measurements. It is noticed that the barrier height is 0.70 eV under reverse bias of −0.2 V. This low value may be attributed to image-force lowering when the junction is under reverse bias.

The barrier height can also be determined with *C–V* measurements, in which the capacitance of a sample is determined through the measured impedance using a suitable equivalent circuit [15]. However, it has been shown that *C–V* measurements with a single alternating current (AC) frequency often produce inaccurate results, and multiple-frequency measurements should be used to account for series resistances [16]. In this paper, impedance spectroscopy between 500 Hz and 1 MHz was employed to extract accurate *C–V* curves. Figure 5 shows the reactance spectra of an Al/S-passivated p-type Si(100) junction under different direct current (DC) bias, in which the time constant at each DC bias produces a maximum in negative reactance at its characteristic resonant frequency. The sample has two space charge regions, as the back contact is Schottky as well. Under forward bias, however, the front contact is in depletion and the back contact is in accumulation. The reactance spectra are dominated by the front contact. Therefore, the maxima in Fig. 5 yield the *C–V* curve and thus the barrier height for the front Al contact [15]. The capacitance is extracted from the maxima using the following equations [15]

$$R = -2X\omega_R \tag{2}$$

$$C = \frac{1}{\omega_R R}, \tag{3}$$

where X is the reactance and ω_R is the resonant frequency.

It is noted that the DC voltage applied in the *C–V* measurement is divided between the series resistance and the space charge region of the Schottky junction, and only the voltage drop in the space charge region should be used for *C–V* measurements. However, with the series resistance at ~30 Ω and the current in the 10^{-7} A/cm^2 range, the

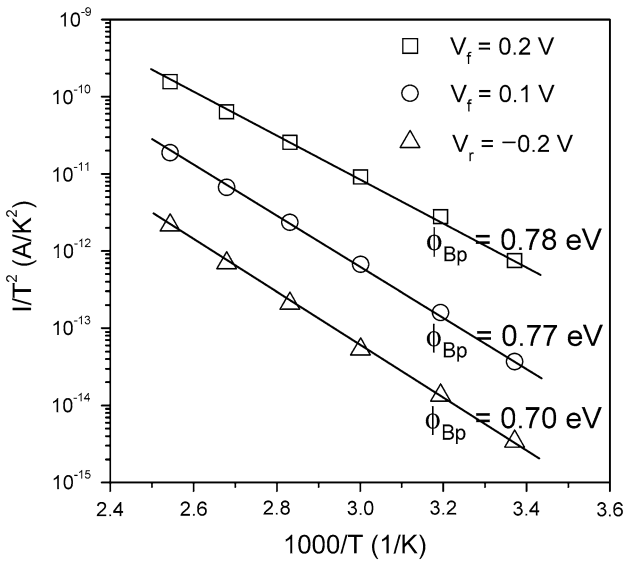

Fig. 4 Activation-energy measurements of an Al/S-passivated p-type Si(100) junction under different bias. The smaller barrier height under reverse bias is due to image-force lowering

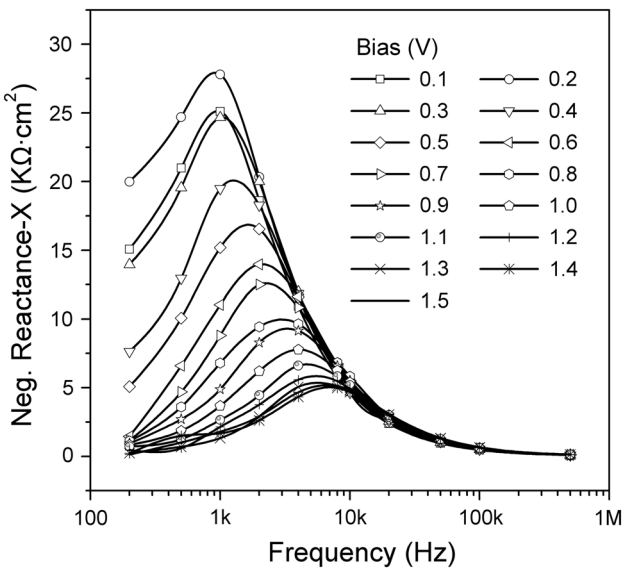

Fig. 5 Reactance spectra of an Al/S-passivated p-type Si(100) junction under different DC bias as a function of frequency. The bias conditions eliminate the effect of the back Schottky contact

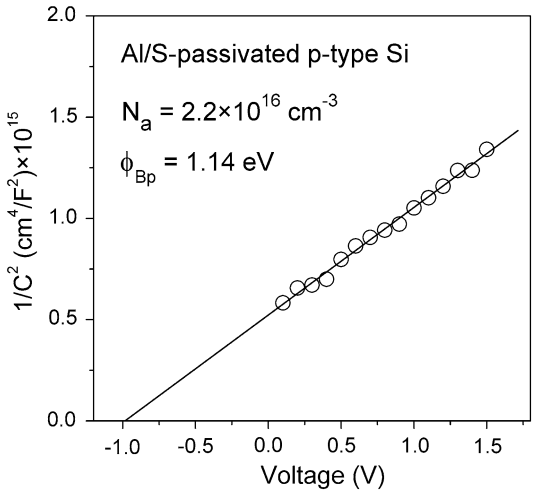

Fig. 6 *C–V* characteristics of an Al/S-passivated p-type Si(100) junction from impedance spectroscopy. A barrier height of 1.14 eV is obtained, suggesting a larger than bandgap barrier

voltage drop on the series resistance is negligibly small. A plot of $1/C^2$ versus corrected DC voltage is presented in Fig. 6. The extracted doping concentration of the wafer is $\sim 2.2 \times 10^{16}$ cm^{-3}, in agreement with the wafer specification (2×10^{16} cm^{-3}). Although sulfur can act as a donor in Si [17], the extracted doping concentration and the straight line in Fig. 6 show no sign of sulfur diffusion into the Si wafer. The extrapolated intercept with the voltage axis is 0.98 V, which represents the amount of surface band bending or surface potential φ_s with zero bias on the junction. For p-type Si with 2.2×10^{16} cm^{-3} doping concentration, the energy difference ϕ_p between Fermi-level E_f and valence band E_v in the bulk is ~ 0.16 eV. With $\phi_{Bp} = \varphi_s + \phi_p + kT/q$, the flat-band Schottky barrier height ϕ_{Bp} for Al/S-passivated p-type Si(100) junctions is thus 1.14 eV. This value is a little higher than our previous report, 1.1 eV, for an Al/p-type Si(100) junction with solution-based sulfur passivation [10]. As the bandgap of Si is 1.12 eV at room temperature, this value suggests that larger than bandgap Schottky barriers are possible.

The apparent 1.14 eV Schottky barrier raises several questions. First of all, *C–V* measurements resulted in a value much higher than *I–V* and activation-energy measurements, 1.14 versus 0.78 eV. Second, the reverse current density of Al/S-passivated p-type Si(100) junctions is in the 10^{-7} A/cm^2 range (Fig. 3), way too high for a 1.14 eV barrier. Finally, the theoretical barrier height for Al/p-type Si junctions is 0.89 eV. This is calculated from the bandgap of Si E_g, 1.12 eV, the electron affinity of Si χ_s, 4.05 eV [18], and the work function of Al ϕ_m, 4.28 eV, through $\phi_{Bp} = E_g + \chi_s - \phi_m$. These questions are discussed in the following sections.

3.3 Dipole moment in S-passivated Si(100) surface

The discrepancy between the measured flat-band barrier height 1.14 eV by *C–V* and the theoretical barrier height 0.89 eV may be attributed to the S–Si dipole moment in the S-passivated surface. The change in barrier height $\Delta\phi_B$ due to surface dipole is given by [10]

$$\Delta\phi_B = \frac{qpN_S}{\varepsilon_r\varepsilon_o}, \tag{4}$$

where ε_o is the permittivity of vacuum, ε_r is the relative permittivity of Si near the interface, which is about half of the bulk Si permittivity [19], often taken as 4 [10, 20]. N_S is the atomic density of sulfur on the Si(100) surface. Assuming a complete monolayer of sulfur, N_S is 6.78×10^{14} atoms/cm^2. p is the dipole moment and can be written as

$$p = d\Delta\rho, \tag{5}$$

where $\Delta\rho$ is the ionic character and d is the separation between the sulfur monolayer and the Si(100) surface, taken as 1.09 Å [10, 21]. Since the S–Si bond is largely covalent (<15 % ionic) [22], the ionic character $\Delta\rho$ may be described by a revised version of Pauling's correlation [23]

$$\Delta\rho = 0.16|X_A - X_B| + 0.035(X_A - X_B)^2, \tag{6}$$

where X_A and X_B are the electro negativities of the atoms involved. For sulfur, it is 2.58 and for Si, it is 1.9. The calculated $\Delta\rho$ is thus 0.12 e. On the S-passivated Si(100) surface, each sulfur atom bonds to two surface Si atoms and vice versa, so for a single S–Si bond, $\Delta\rho$ is 0.06 e. Using the above parameters, the calculated $\Delta\phi_B$ is 0.2 eV, which accounts for the discrepancy between the measured flat-band barrier height and the theoretical barrier height.

3.4 Image force-induced barrier lowering

A 1.14-eV barrier should produce an extremely small reverse current density in the range of 10^{-11} A/cm^2. The actual reverse current density from *I–V* measurements is 3.9×10^{-7} A/cm^2 at 300 K (Fig. 3). This discrepancy may be attributed to image force-induced lowering of the barrier and the leakage current along the edge of the Al contacts. In our previous work [10], a barrier height of 1.1 eV for an Al/S-passivated p-type Si(100) junction resulted in weakly degenerate inversion on the Si surface, and a 0.08 eV image-force lowering was concluded from a surface electric field of 2×10^5 V/cm. In this work, the barrier height of 1.14 eV from *C–V* indicates stronger inversion on the Si surface. The presence of this stronger inversion induces a higher electrical field near the Si surface, resulting in more lowering of the barrier height. The

electric field on a surface of inversion can be written as [24]

$$E_S = \pm \frac{\sqrt{2}kT}{qL_D} F\left(\frac{q\phi_s}{kT}, \frac{n_{po}}{p_{po}}\right), \tag{7}$$

where n_{po} and p_{po} are the equilibrium concentrations of electrons and holes in p-type Si. L_D is the extrinsic Debye length for holes and is given by

$$L_D = \sqrt{\frac{kT\varepsilon_r\varepsilon_o}{q^2 p_{po}}}, \tag{8}$$

where ε_r is the relative permittivity of Si. Another abbreviation in Eq. 7

$$F\left(\frac{q\phi_s}{kt}, \frac{n_{po}}{p_{po}}\right) = \sqrt{\left(e^{-q\phi_s/kT} + \frac{q\phi_s}{kT} - 1\right) + \frac{n_{po}}{p_{po}}\left(e^{q\phi_s/kT} - \frac{q\phi_s}{kT} - 1\right)}, \tag{9}$$

where ε_s is the surface potential, taken as 0.98 V from the *C–V* measurement. With these parameters, a surface electric field E_S of 1.57×10^6 V/cm is obtained. Such a high electric field results in significant image-force lowering [24]

$$\Delta\varphi = \sqrt{\frac{q|E_S|}{4\pi\varepsilon_r\varepsilon_o}} \tag{10}$$

The image-force lowering calculated is as high as 0.24 eV. This barrier lowering is experienced by charge carriers moving across the interface in *I–V* measurements. It does not occur under flat band where *C–V* extracts the barrier height [25]. This is why the barrier height from *C–V* is higher than *I–V* and activation-energy measurements.

3.5 Edge-leakage current

The calculated image-force lowering above accounts for only part of the barrier height difference between *C–V* and *I–V* measurements. Another reason for the higher than expected reverse current density in the *I–V* measurement is the leakage current, which is caused by the high electric field around the periphery of the Al contacts. If the reverse current is dominated by thermionic emission (Eq. 1), it is proportional to the area of the Al contact, i.e., a quadratic relation between current and contact diameter. On the other hand, if the reverse current is dominated by edge effects, it is proportional to the circumference of the Al contact, i.e., a linear relation between current and contact diameter [24]. Figure 7 shows the reverse current of Al/S-passivated p-type Si(100) junctions as a function of the diameter of the Al contacts from 600 to 1,200 μm. The reverse current increases neither linearly nor quadratically with the diameter of the Al contact, suggesting that the reverse current is

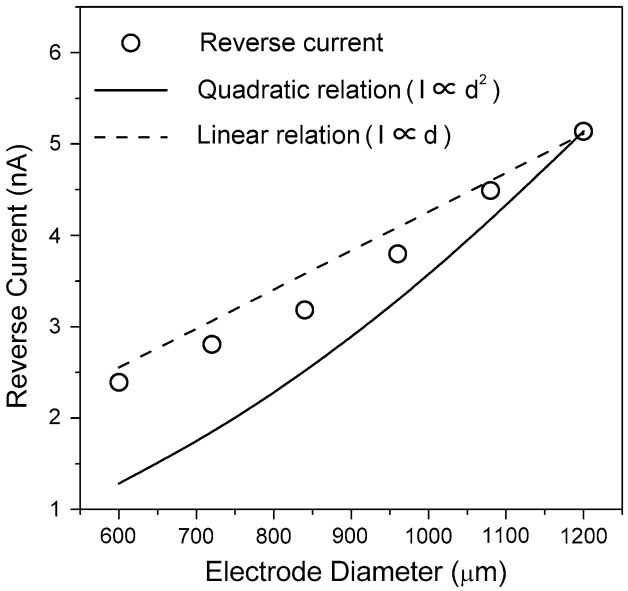

Fig. 7 Reverse current of Al/S-passivated p-type Si(100) junctions as a function of Al contact diameter. The largely linear relationship indicates significant edge-leakage current

neither 100 % edge-leakage current nor 100 % thermionic emission current. However, the reverse current is more linear than quadratic, indicating that it is largely edge-leakage current. The edge-leakage current produces a larger reverse current and reduces the apparent barrier height in *I–V* measurements.

3.6 Thermal stability of sulfur passivation

The thermal stability of Al/S-passivated Si(100) junctions was determined by monitoring their *I–V* behavior before and after annealing. Figure 8 shows the *I–V* characteristics of Al/S-passivated p-type Si(100) junctions before and after annealing at 300 °C for 30 s in air. Before annealing the reverse current density at 0.5 V is 5.1×10^{-7} A/cm^2. After annealing, it increases to 9.1×10^{-7} A/cm^2. The relatively small change in reverse current density suggests a thermally stable high Schottky barrier up to 300 °C. This is in sharp contrast to the poor thermal stability of the 1.1 eV barrier in our previous report [10], in which the high Schottky barrier disappeared after annealing to just 150 °C. The thermal stability of the metal/valence-mended Si(100) junctions is due to the suppressed chemical reactivity of the Si(100) surface by valence-mending passivation [26]. The better thermal stability by CVD suggests better passivation quality over the previous solution passivation.

Figure 9 shows the *I–V* characteristics of Al/S-passivated n-type Si(100) junctions immediately and 47 days after fabrication, and then annealed at different temperatures from 300 to 500 °C. The junctions remain ohmic all

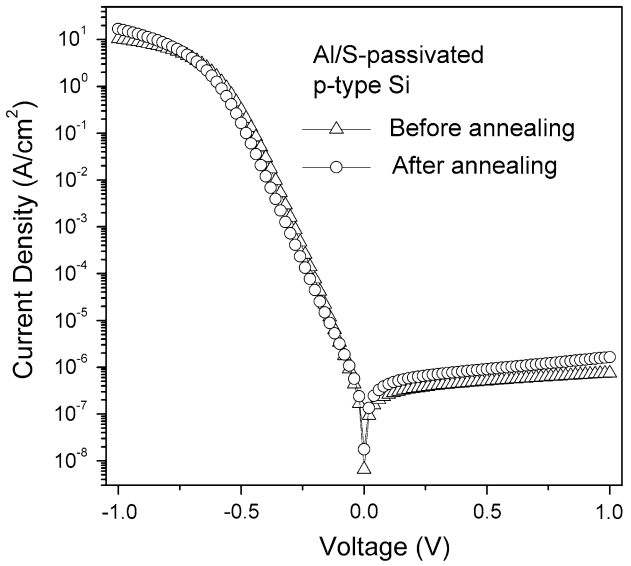

Fig. 8 I–V characteristics of Al/S-passivated p-type Si(100) junctions before and after annealing at 300 °C in air for 30 s. The junctions are thermally stable to 300 °C

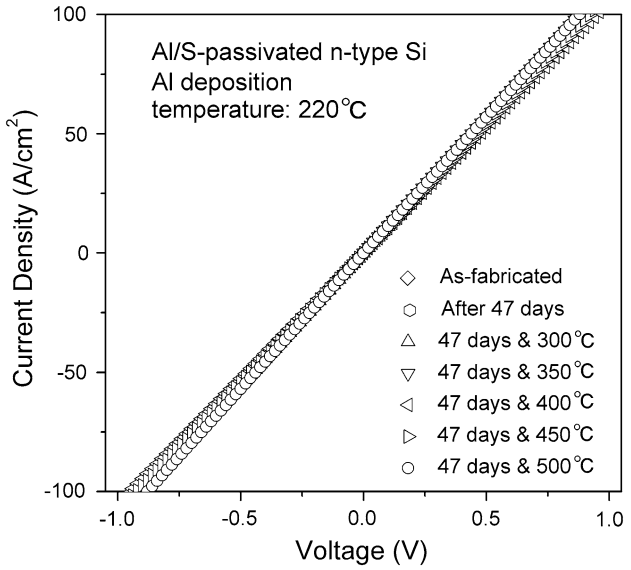

Fig. 9 I–V characteristics of Al/S-passivated n-type Si(100) junctions immediately and 47 days after fabrication, and then annealed at different temperatures. The Al contacts are deposited at 220 °C

the way to 500 °C. One difference between these samples and all other samples in this paper is that the deposition of the Al contacts is performed at a substrate temperature of 220 °C in the electron-beam evaporator. In our previous work it was noted that there is a layer of adsorbate sandwiched between the valence-mended Si(100) surface and the Al layer when the valence-mended sample is exposed to air (data not shown). The oxygen in the adsorbate layer can react with the sulfur passivation layer at elevated temperatures and damage the passivation. It is suggested that by heating the substrate, the adsorbates are driven off from the surface and a cleaner Al/S-passivated Si(100) interface is obtained, leading to significantly better thermal stability.

4 Conclusion

Surface states between Al and Si(100) surface are significantly reduced by CVD-based sulfur passivation on both n-type and p-type Si(100) wafers. Al/S-passivated n-type Si(100) junctions exhibit ohmic behavior with a barrier height of less than 0.078 eV by the *I–V* method and significantly lower than 0.08 eV by the activation-energy method. For Al/S-passivated p-type Si(100) junctions, the barrier height is $\sim$0.77 eV by *I–V* and activation-energy methods and 1.14 eV by the *C–V* method. The discrepancy between *C–V* and other methods is explained by image force-induced barrier lowering and edge-leakage current. Further research is needed to minimize image-force lowering and edge-leakage current to reduce the reverse current density for the 1.14-eV Schottky junction. The *I–V* behavior of an Al/S-passivated p-type Si(100) junction remains largely unchanged after 300 °C annealing in air. It is also discovered that heating the S-passivated Si(100) wafer before Al deposition significantly improves the thermal stability of an Al/S-passivated n-type Si(100) junction to 500 °C.

Acknowledgments This work was supported by the US Department of Energy through the SunShot Program under Grant No. DE-EE-0005322.

References

1. E. Simoena, C. Gong, N. Posthuma, E. Kerschaver, J. Poortmans, R. Mertens, J. Electrochem. Soc. **158**, H612 (2011)
2. A.G. Aberle, Prog. Photovolt. Res. Appl. **8**, 473 (2000)
3. Tao M., Conference Records of 33rd IEEE Photovoltaic Specialist Conference (San Diego, 2008)
4. A.G. Aberle, Sol. Energy Mater. Sol. Cells **65**, 239 (2001)
5. J. Schmidt, M. Kerr, A. Cuevas, Semicond. Sci. Technol. **16**, 164 (2001)
6. B. Hoex, J.J.H. Gielis, M.C.M. van de Sanden, W.M.M. Kessels, J. Appl. Phys. **104**, 113703 (2008)
7. G. Dingemans, P. Engelhart, R. Seguin, F. Einsele, B. Hoex, M.C.M. van de Sanden, W.M.M. Kessels, J. Appl. Phys. **106**, 114907 (2009)
8. E. Kaxiras, Phys. Rev. B **43**, 6824 (1991)
9. M. Tao, S. Agarwal, D. Udeshi, N. Basit, E. Maldonado, Appl. Phys. Lett. **83**, 2593 (2003)
10. G. Song, M.Y. Ali, M. Tao, IEEE Electron. Dev. Lett. **28**, 71 (2007)
11. M. Tao, D. Udeshi, N. Basit, E. Maldonado, W.P. Kirk, Appl. Phys. Lett. **82**, 1559 (2003)
12. E. Dubois, G. Larrieu, J. Appl. Phys. **96**, 729 (2004)

13. A.M. Cowley, S.M. Sze, J. Appl. Phys. **36**, 3212 (1965)
14. A.I. Prokopyev, S.A. Mesheryakov, Measurement **33**, 135 (2003)
15. K.M. Guenther, H. Witte, A. Krost, S. Kontermann, W. Schade, Appl. Phys. Lett. **100**, 042101 (2012)
16. J.F. Lønnum, J.S. Johannessen, Electron. Lett. **22**, 456 (1986)
17. K.M. Guenther, T. Gimpel, S. Kontermann, W. Schade, Appl. Phys. Lett. **102**, 202104 (2013)
18. R. Hunger, R. Fritsche, B. Jaecke, W. Jaegermann, Phys. Rev. B **72**, 045317 (2005)
19. H.B. Michaelson, J. Appl. Phys. **48**, 4729 (1977)
20. R. Ludeke, G. Jezequel, A. Taleb-Ibrahim, Phys. Rev. Lett. **61**, 601 (1998)
21. A. Papageorgopoulos, A. Corner, M. Kamaratos, C.A. Papageorgopoulos, Phys. Rev. B **55**, 4435 (1997)
22. N.B. Annay, C. Smyth, J. Am. Chem. Soc. **68**, 171 (1946)
23. T.U. Kampen, W. Moinch, Surf. Sci. **331–333**, 490 (1995)
24. S.M. Sze, K.K. Ng, *Physics of semiconductor device*, 3rd edn. (Wiley, New York, 2007)
25. van Zeghbroeck B., Principles of semiconductor devices (Colorado Press, 2011)
26. J. Shanmugam, J.G. Zhu, Y. Xu, W.P. Kirk, M. Tao, IEEE Trans. Electron. Devices **53**, 719 (2006)